

Article

# Spatial Variations in the Abundance and Chemical Speciation of Phosphorus across the River–Sea Interface in the Northern Beibu Gulf

Bin Yang <sup>1,2</sup> , Zhen-Jun Kang <sup>1,2</sup>, Dong-Liang Lu <sup>1,\*</sup>, Solomon Felix Dan <sup>3</sup>, Zhi-Ming Ning <sup>4</sup> , Wen-Lu Lan <sup>5</sup> and Qiu-Ping Zhong <sup>1</sup>

<sup>1</sup> Guangxi Key Laboratory of Marine Disaster in the Beibu Gulf, Qinzhou University, Qinzhou 535011, China; binyang@qzhu.edu.cn (B.Y.); zjkang@qzhu.edu.cn (Z.-J.K.); zhqp02@163.com (Q.-P.Z.)

<sup>2</sup> Key Laboratory of Coastal Science and Engineering, Beibu Gulf, Qinzhou 535011, China

<sup>3</sup> Key Laboratory of Marine Chemistry Theory and Technology, Ministry of Education, Ocean University of China, Qingdao 266100, China; solomon.dan86@yahoo.com

<sup>4</sup> School of Marine Sciences, Guangxi University, Nanning 530004, China; zmning@gxu.edu.cn

<sup>5</sup> Marine Environmental Monitoring Center of Guangxi, Beihai 536000, China; dr.lan@139.com

\* Correspondence: ldl@qzhu.edu.cn; Tel.: +86-777-2808363

Received: 8 June 2018; Accepted: 12 August 2018; Published: 18 August 2018



**Abstract:** Water samples were collected to measure dissolved and particulate phosphorus species in order to examine the dynamics of phosphorus in the water column across the river–sea interface from the lower Dafengjiang River to the open Beibu Gulf. Dissolved inorganic phosphorus concentrations were as high as  $0.90 \pm 0.42 \mu\text{M}$  in river water but decreased dramatically to as low as  $0.02 \pm 0.01 \mu\text{M}$  in open coastal waters. Total dissolved phosphorus was largely measured in the form of dissolved inorganic phosphorus in river waters ( $58\% \pm 18\%$ ), whereas dissolved organic phosphorus became the predominant species ( $>90\%$  on average) in open coastal waters. Total dissolved phosphorus was the dominant species, comprising  $76\% \pm 16\%$  of the total phosphorus, while total particulate phosphorus only comprised  $24\% \pm 16\%$  of the total phosphorus pool. Riverine inputs, physical and biological processes, and particulate phosphorus regeneration were the dominant factors responsible for the dynamic variations of phosphorus species in the study area. Based on a two-end-member mixing model, the biological uptake resulted in a dissolved inorganic phosphorus depletion of  $0.12 \pm 0.08 \mu\text{M}$  in the coastal surface water, whereas the replenishment of dissolved inorganic phosphorus in the lower river from particle P regeneration and release resulted in an increase ( $0.19 \pm 0.22 \mu\text{M}$ ) of dissolved inorganic phosphorus in the estuarine mixing region. The molar ratios of dissolved inorganic nitrogen to dissolved inorganic phosphorus and dissolved silicate to dissolved inorganic phosphorus in the open surface waters were  $>22$ , suggesting that, although the lower Dafengjiang River contained elevated concentrations of dissolved inorganic phosphorus, the northern Beibu Gulf was an overall P-limited coastal ecosystem.

**Keywords:** phosphorus; chemical speciation; nutrient; Dafengjiang River; Beibu Gulf

## 1. Introduction

Phosphorus (P) is an essential macronutrient to the growth of phytoplankton and plays a vital role in regulating the primary productivity and water quality in aquatic environments [1–3]. The geochemical cycling and bioavailability of P depend mainly on the chemical species of P in freshwater and marine ecosystems [4,5]. Different chemical species of P play different roles in the bioavailability and geochemical cycling of P in the water column [6,7]. Thus, knowledge of the abundance and chemical speciation of P in aquatic systems are the keys to better understanding the

dynamics of P and its role in regulating water quality in coastal marine environments [8,9]. P in natural waters occurs in both dissolved or particulate as well as inorganic or organic forms. Dissolved inorganic P (DIP) can be assimilated and utilized preferentially by a wide range of living organisms [10] and thus play an important role in regulating different biological processes [11]. Studies have shown that dissolved organic P (DOP) could also be a potential source of P for biological communities [12–14], especially when the supply of DIP is deficient for biomass growth [15,16]. Recently, it has been shown that both phytoplankton and bacteria can utilize DOP through a variety of phosphatase enzymes such as alkaline phosphatase, which has been used as an indicator of P stress [17–19].

More than 90% of P carried by rivers to estuaries and coastal waters are closely associated with suspended particulate matter [20]. Therefore, particle-bound P is expected to be a significant fraction of P in estuarine and coastal environments. The total particulate P (TPP) is a complex intermediate compound bounded by P derivatives of both nonbiogenic and biogenic particulate forms [9]. The nonbiogenic TPP has high affinity to clay or rock fragments and have less significance for biological processes [20]. On the other hand, biogenic TPP, i.e., living and dead plankton biomass or cells, can be remineralized into DOP or recycled within the water column [21]. Approximately 20% of TPP that is adsorbed onto particulate matter in estuaries can be dissolved in the form of DIP, which can be enhanced by biogeochemical processes in the water column [22]. Moreover, the dissolution of DIP from particulate matter can be improved with increasing salinity [23]. In addition, TPP that is bound to oxidized Fe species may release DIP into the water column when Fe oxides/hydroxides are reduced from suspended particulate matter and sediments [24,25]. This process boosts DIP availability in aquatic environments [26]. Therefore, TPP can also be a potential source of P for the growth of phytoplankton in estuarine and marine phytoplankton. Thus, it is necessary to evaluate the contributions of particulate P in addition to DIP to the total P pool in the riverine, estuarine, and coastal waters, especially in P-limited environments.

Due to the increasing influence of anthropogenic activities and climate change in the Chinese coastal regions, many estuaries are affected by eutrophication, harmful algal blooms, seasonal hypoxia, and nutrient pollution [27–29]. The Dafengjiang River estuary (DRE) is a shallow estuarine system on the coast of Guangxi Province, China. The distribution of DIP in the DRE has been recently reported [30,31]. Nevertheless, there is a knowledge gap on the dynamics of DOP and TPP in the region. The Qinzhou Bay has been shown to be a potential P-limited ecosystem [32]. However, little is known about the variations in the abundance and partitioning of inorganic and organic P species in the Dafengjiang River and its estuary.

Our main research objectives were: (1) to quantify the abundance different P species from surface to bottom waters and their dynamic changes across the river–sea interface from the lower Dafengjiang River to the open Beibu Gulf; (2) to elucidate the partitioning of P species between dissolved and particulate phases and their transformation along the river–seawaters; and (3) to examine the mixing behavior of DIP and factors controlling the dynamics of P species at the river–sea interface.

## 2. Materials and Methods

### 2.1. Study Area

The Dafengjiang River estuary is located at the south coast of the Guangxi province, China; it is a shallow estuary connecting to Qinzhou Bay and the Beibu Gulf (Figure 1a). The Dafengjiang River is a small river compared to most of the well-studied rivers in China and worldwide. It has a length of 185 km and watershed area of 1927 km<sup>2</sup> with an average water depth of ~7 m [33]. Annual average freshwater discharge is  $18.3 \times 10^9$  m<sup>3</sup>, and approximately  $11.77 \times 10^4$  tons of suspended sediments are loaded to the estuary [33]. More than 80% of the freshwater is discharged in flood season, i.e., from April to September, when the southwestern monsoon prevails. The remaining 20% is discharged in the dry season, i.e., from October to March [34]. The estuary, which is somewhat triangular in shape, develops a main stream debouching into the open Beibu Gulf in the northwestern South China Sea (Figure 1a).

The coast is subjected to diurnal macro tides with a typical tidal range of 5.7 m [35]; the tidal excursion sometimes extends upstream to a length of ~60 km. The islands within the estuary and fringes of the riversides up to 6 km upstream are dominated by mangrove vegetation. These forests areas are predominated by dwarf *Aegiceras corniculatum* comm. intermixed with patches of *Avicennia marina* comm. and *Kandelia candel* comm. [36].

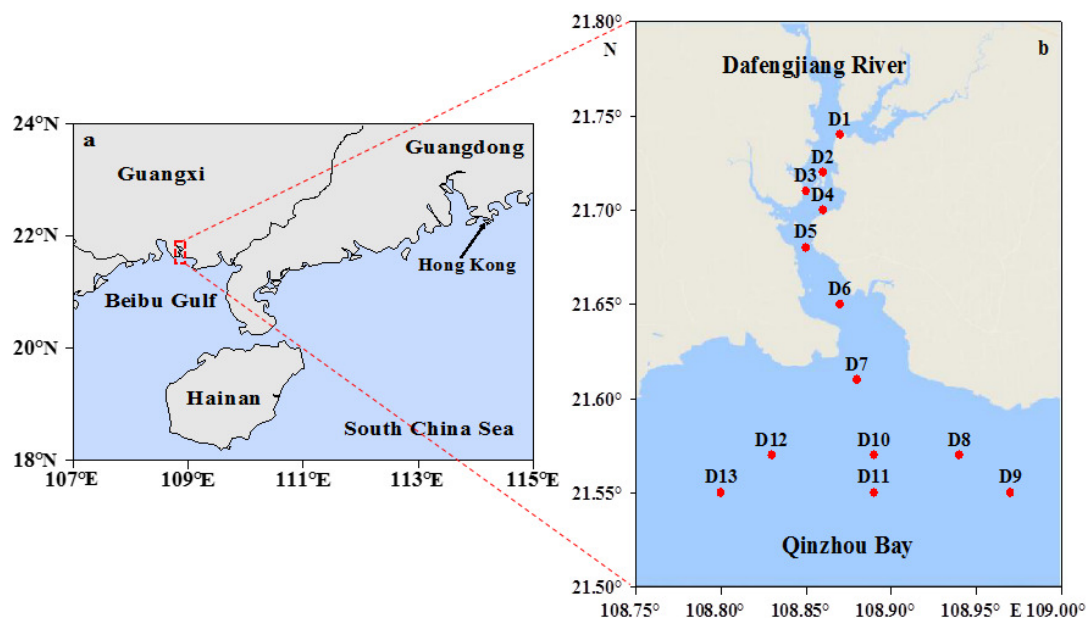


Figure 1. Map showing (a) the study station location and (b) sampling stations.

Anthropologic activities in the catchment area are predominated by agriculture. Rice and sugar cane are the main crops in Guangxi, which has become the largest producer of sugar cane in China [37]. Wood produce from eucalyptus is a rapidly growing sector of agriculture [38]. Shrimp and fish pond aquacultures are located at the landward part of the estuary, with pond area exceeding 1000 ha (Huai-Yi Fang, personal communication). During the winter season, these shrimp and fish ponds are fallowed; the discharge of pond, water is limited to the two short harvest periods during the summer and autumn. Such management is quite different from the other regions in China [39,40] and Southeast Asia [41], where water is repeatedly exchanged over all the production cycle due to limited arable farming in the winter.

## 2.2. Sampling

As previously mentioned, restricted anthropogenic activities such as aquaculture and arable farming are predominant in winter (dry) season with limited riverine inputs in the study area. Field sampling was carried out in December 2017 to examine specific physical, chemical, or biological processes controlling the dynamics of P species in the water column. Sampling stations are shown in Figure 1b. Water samples were collected at six stations (D8–D13) in the Qinzhou Bay on 24 December 2017, and seven stations (D1–D7) were sampled on 25 December 2017 in the lower Dafengjiang River during high tide. At each station, both surface (~0.5 m depth) and near bottom (~2 m above the sediment) water samples were collected with a polymethyl methacrylate water sampler ( $V = 5$  L). A multiparameter water quality probe (AP-5000, Aquaread Co., Kent, UK) was used to measure water temperature (T), salinity (S), pH, and dissolved oxygen (DO) during sampling. Samples were filtered through a 0.45  $\mu\text{m}$  Nuclepore filter (Whatman, 47 mm) for the measurements of nitrate ( $\text{NO}_3^-$ ), nitrite ( $\text{NO}_2^-$ ), ammonium ( $\text{NH}_4^+$ ), dissolved silicate (DSi), dissolved inorganic phosphorus (DIP), and total dissolved phosphorus (TDP). Dissolved inorganic nitrogen (DIN) was the sum of  $\text{NO}_3^-$ ,  $\text{NO}_2^-$ , and  $\text{NH}_4^+$ . The filter samples were used to measure total particulate phosphorus

(TPP). An aliquot of 300–500 mL water samples for chlorophyll *a* (Chl-*a*) analysis was filtered through pre-combusted Whatman GF/F filters. The filtrates and filters were stored in the dark on ice during field excursions and then immediately stored at  $-20\text{ }^{\circ}\text{C}$  in the laboratory until analysis within two weeks.

### 2.3. Analytical Methods

The concentrations of  $\text{NO}_3^-$  and  $\text{NH}_4^+$  were determined using the Cu–Cd column reduction and the indophenol blue color formation methods, respectively [42]. The analysis of  $\text{NO}_2^-$  was based on the reaction of an aromatic amine with  $\text{NO}_2^-$ ; the reaction product was quantified using spectrophotometric methods [42]. DIP was measured according to the spectrophotometric phosphomolybdate blue method [43]. TDP was determined as DIP after digestion of the samples with acidified  $50\text{ g L}^{-1}$   $\text{K}_2\text{S}_2\text{O}_8$  solution ( $\text{pH} = 1$ ) in an autoclave sterilizer at  $125\text{ }^{\circ}\text{C}$  for 90 min [44]. DOP was obtained from the difference between TDP and DIP (i.e.,  $\text{DOP} = \text{TDP} - \text{DIP}$ ) [6]. DSi was measured with molybdate, oxalic acid, and a reducing reagent [42]. The analytical precision was  $<5\%$  for  $\text{NO}_3^-$ ,  $\text{NO}_2^-$ ,  $\text{NH}_4^+$ , TDP, DIP, and DSi [45].

TPP was measured using the methods of Aspila et al. (1976) [46]. The filters were first wetted with  $0.5\text{ M}$   $\text{MgCl}_2$  solution and heated in an oven at  $95\text{ }^{\circ}\text{C}$  until dry, followed by ashing in a furnace at  $550\text{ }^{\circ}\text{C}$  for 2 h and then extracted using  $1\text{ M}$   $\text{HCl}$  solution at room temperature for 24 h. The analytical precision of TPP was  $<5\%$  [45]. The concentration of total phosphorus (TP) was calculated as the sum of TDP and TPP (i.e.,  $\text{TP} = \text{TDP} + \text{TPP}$ ) [7].

Chl-*a* on the filter was extracted using  $10\text{ mL}$   $90\%$  (*v/v*) acetone at  $4\text{ }^{\circ}\text{C}$  in the dark for 24 h, and the extractions were analyzed using a fluorescence spectrophotometer (F-4500, Hitachi Co., Tokyo, Japan) after centrifugation, according to the procedure of Parsons et al. (1984) [47]. The analytical precision was  $<3\%$  for Chl-*a* analysis.

### 2.4. Two-End-Member Mixing Model

The two-end-member mixing model was based on mass balance equations for the component of two water masses and salinity [7]:

$$f_1 + f_2 = 1 \quad (1)$$

$$S_1 f_1 + S_2 f_2 = S \quad (2)$$

where  $f_1$  and  $f_2$  are the components of the freshwater and seawater, respectively.  $S_1$  and  $S_2$  are the salinity of two end-member samples. Therefore, adopting the above two-end-member model, the specific P concentration ( $P_m$ ) in waters of the study area was calculated based on the following equation:

$$P_m = P_1 f_1 + P_2 f_2 \quad (3)$$

where  $P_1$  and  $P_2$  are the specific P concentration of the two end-members. The  $\Delta P$  is defined as the difference between the theory model value and the ambient value:

$$\Delta P = P_m - N \quad (4)$$

where  $N$  denotes the ambient P concentration in the water sample. A positive value of  $\Delta P$  suggests DIP removal, while a negative value suggests DIP addition.

### 2.5. Statistical Analysis

In the present study, all data, unless mentioned otherwise, were reported as an average  $\pm$  standard deviation (SD). Pearson's correlation analysis with a two-tailed test of significance analysis was conducted using the Statistical Package for Social Sciences (SPSS) for Windows (Version 20.0; SPSS Inc., IBM, Armonk, NY, USA) to study the relationship between the environmental parameters. A Person test analysis was carried out to ascertain significant differences ( $p < 0.05$ ) between datasets. Additionally,

this program was also applied to run one-way analysis of variance (ANOVA) to ascertain whether the spatial variations of P species are statistically significant at the 95% confidence level. In factor analysis, the varimax rotation method and principal component analysis (PCA) were applied for extraction and for deriving principal components, respectively. Generally, the number of factors in the PCA model is defined by considering only those the eigenvalues of which are  $>1$  [48].

### 3. Results

#### 3.1. Environmental Parameters

In the present study, surface water temperatures varied from 15.61 to 16.21 °C (average,  $15.82 \pm 0.19$  °C) and 15.50 to 15.90 °C (average,  $15.61 \pm 0.12$  °C) in the bottom water (Table 1), suggesting a well-mixed water column without stratification during the study period. Salinity in surface water ranged from 18.38 to 26.61 psu (average,  $23.73 \pm 2.66$  psu) and 19.08 to 26.81 psu (average,  $24.28 \pm 2.42$  psu) in bottom water (Table 1). The ranges of pH in surface and bottom waters were 8.12–8.63 (average,  $8.43 \pm 0.19$ ) and 8.26–8.65 (average,  $8.47 \pm 0.16$ ), respectively (Table 1). DO concentrations were usually  $>9$  mg L<sup>-1</sup> both in the surface and bottom waters (Table 1). This reflected the characteristics of aerobic water during the study period. Although the lower coefficient of variation (CV) of temperature (1.2%) and pH (2.3%) in surface waters and the CV of temperature (0.8%) and pH (1.9%) in bottom waters indicated very low variations among the samples, they still showed slightly increasing trends from the lower Dafengjiang River to the open Beibu Gulf in the water column (Figure 2a,b,e,f). The CV of salinity was 11% and 10% in surface and bottom waters, respectively, and showed a significant increasing trend from the lower Dafengjiang River to the open Beibu Gulf in the water column (Figure 2c,d). The Chl-*a* concentration of 2.41–6.96 µg L<sup>-1</sup> (average,  $4.44 \pm 1.76$  µg L<sup>-1</sup>) at the surface water was relatively high compared to that of the bottom water (average,  $3.91 \pm 1.22$  µg L<sup>-1</sup>) (Table 1). Chl-*a* generally had a similar distribution to salinity both in the surface and bottom waters (Figure 2c,d,g,h), with a strong influence from biological production at the southwestern part of the DRE.

**Table 1.** Sampling locations, station, water depth, temperature, salinity, pH, dissolved oxygen, and chlorophyll *a* (Chl-*a*) in the Dafengjiang River estuary during December 2017.

Sample Locations	Site	Longitude (°E)	Latitude (°N)	Depth (m)	Temperature (°C)	Salinity (psu)	pH	DO (mg L <sup>-1</sup> )	Chl- <i>a</i> (µg L <sup>-1</sup> )
Surface Waters									
Lower Dafengjiang River	D1	108.87	21.74	10.0	15.71	18.38	8.12	9.12	2.52
	D2	108.86	21.72	14.6	15.71	19.97	8.17	9.15	4.90
	D3	108.85	21.71	10.2	15.70	21.04	8.23	9.14	2.72
	D4	108.86	21.70	8.0	15.68	21.85	8.24	9.15	5.65
	D5	108.85	21.68	7.3	15.70	22.97	8.29	9.08	6.24
	D6	108.87	21.65	6.0	15.72	24.06	8.44	9.05	2.69
	D7	108.88	21.61	11.0	15.78	24.65	8.46	9.18	3.30
Qinzhou Bay	D8	108.94	21.57	6.6	15.75	25.86	8.57	9.82	3.09
	D9	108.97	21.55	6.4	16.11	25.64	8.61	9.93	4.18
	D10	108.89	21.57	6.2	15.81	25.29	8.60	9.66	6.53
	D11	108.89	21.55	6.0	16.21	25.70	8.63	9.80	2.41
	D12	108.83	21.57	5.5	15.61	26.44	8.63	9.67	6.56
	D13	108.80	21.55	6.0	16.11	26.61	8.57	9.58	6.96
Bottom Waters									
Lower Dafengjiang River	D1	108.87	21.74	10.0	15.50	19.08	8.26	9.12	2.75
	D2	108.86	21.72	14.6	15.51	20.91	8.27	9.11	2.93
	D3	108.85	21.71	10.2	15.61	21.79	8.28	9.17	3.51
	D4	108.86	21.70	8.0	15.51	22.88	8.29	9.16	5.07
	D5	108.85	21.68	7.3	15.51	23.90	8.38	9.01	3.13
	D6	108.87	21.65	6.0	15.60	24.48	8.45	9.04	2.52
	D7	108.88	21.61	11.0	15.61	25.68	8.50	9.13	4.39
Qinzhou Bay	D8	108.94	21.57	6.6	15.51	25.92	8.59	9.95	3.50
	D9	108.97	21.55	6.4	15.71	25.97	8.64	9.99	4.24
	D10	108.89	21.57	6.2	15.62	25.82	8.61	9.76	4.55
	D11	108.89	21.55	6.0	15.90	25.92	8.65	9.90	2.41
	D12	108.83	21.57	5.5	15.53	26.47	8.64	9.71	5.60
	D13	108.80	21.55	6.0	15.78	26.81	8.58	9.38	6.28

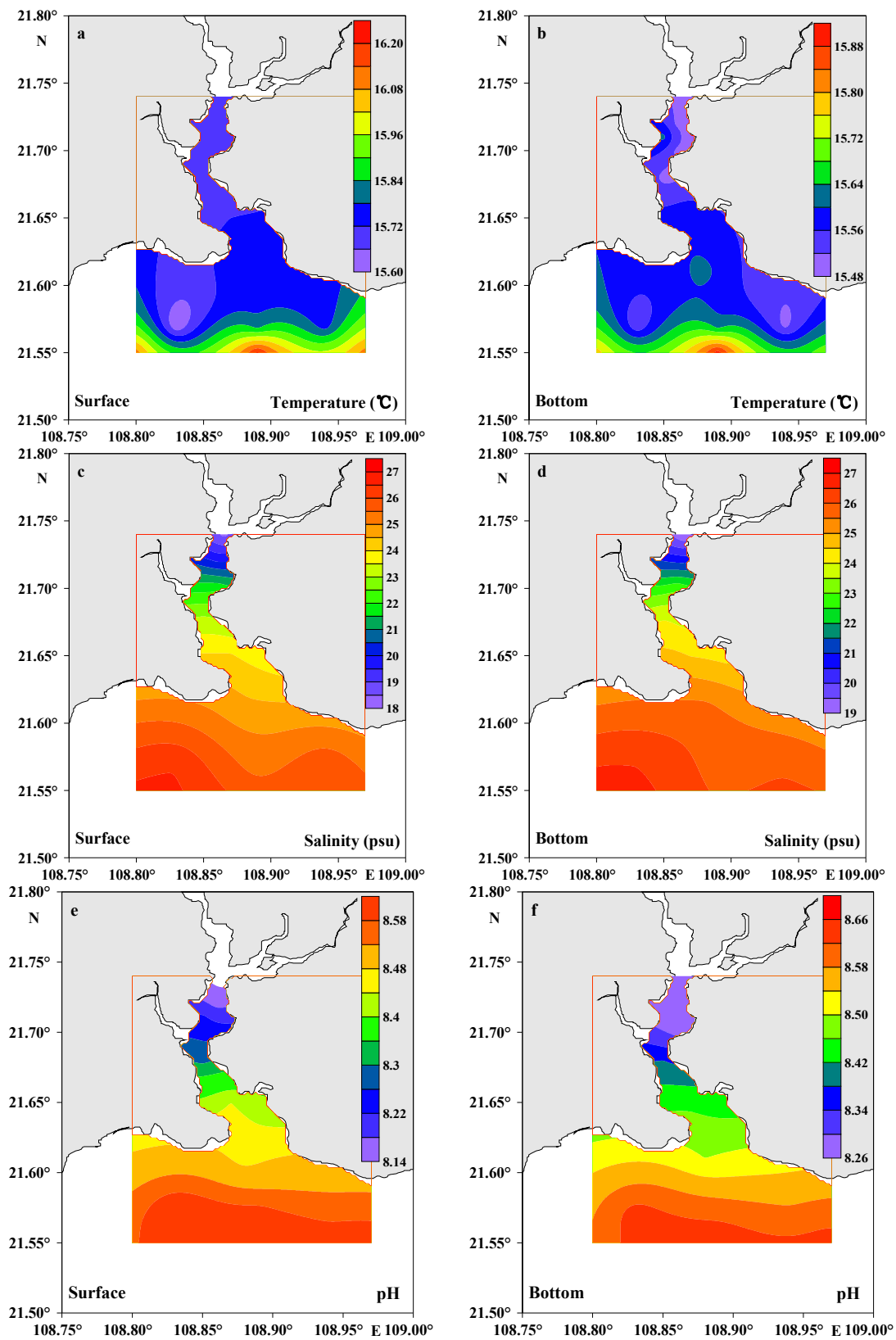
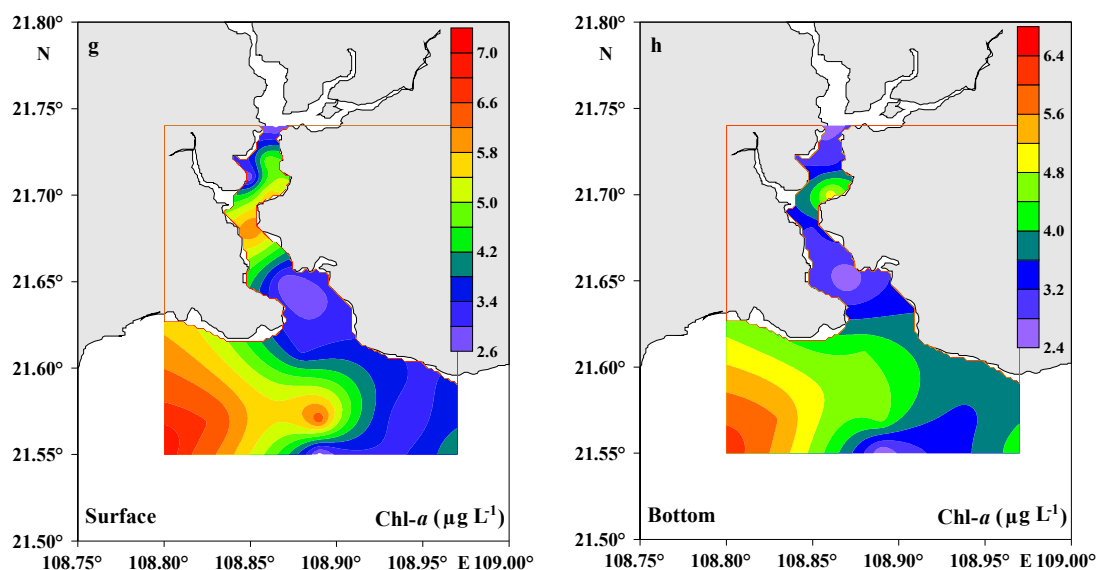


Figure 2. Cont.



**Figure 2.** Distributions of temperature, salinity, pH, and Chl-*a* in surface and bottom waters of the Dafengjiang River estuary.

### 3.2. Spatial Variations of Dissolved Inorganic Nitrogen, Silicate, and Nutrient Ratios

Table 2 summarizes the concentrations of dissolved inorganic nitrogen and silicate in the surface and bottom waters from the lower Dafengjiang River to Qinzhou Bay. Spatial variations of  $\text{NO}_3^-$ , DIN, and DSi concentrations are shown in Figure 3. When salinity showed an increasing trend from the lower Dafengjiang River to Qinzhou Bay, the concentrations of  $\text{NO}_3^-$ , DIN, and DSi both in surface and bottom waters gradually decreased, respectively (Figure 3). This suggests that the DIN and DSi loading to the river estuary were closely related to freshwater discharge and seawater dilution, as indicated by the significant relationship between DIN and DSi vs. salinity (Table 3).  $\text{NO}_3^-$  was the primary component of DIN, which accounted for 52%–78% of DIN in the surface and 50%–81% of DIN in the bottom waters (Table 2, Figure 3). Similar findings have been reported by other investigators in oxygenated waters [49,50]. The molar ratios of DIN/DIP and DSi/DIP in the surface water increased from the lower Dafengjiang River to Qinzhou Bay; variations were between 13–217 and 5–89, respectively (Figure 4). Justić et al. (1995) pointed out that ambient molar ratios of DIN/DIP and DSi/DIP, which are >22 indicates stoichiometric (potential) P limitation for phytoplankton growth [51]. It is interesting to note that both the molar ratios of DIN/DIP and DSi/DIP at stations D8–D13 in the Qinzhou Bay were >22 (Figure 4), suggesting that P could be potentially limiting for primary production in the coastal region, which was similar to previous observation [32].

**Table 2.** Concentrations of  $\text{NO}_2^-$ ,  $\text{NO}_3^-$ ,  $\text{NH}_4^+$ , dissolved inorganic nitrogen (DIN), dissolved silicate (DSi), dissolved inorganic P (DIP), dissolved organic P (DOP), total dissolved phosphorus (TDP), total particulate phosphorus (TPP), and total phosphorus (TP) in surface and bottom waters of the Dafengjiang River estuary.

Sample Locations	Site	$\text{NO}_2^-$ ( $\mu\text{M}$ )	$\text{NO}_3^-$ ( $\mu\text{M}$ )	$\text{NH}_4^+$ ( $\mu\text{M}$ )	DIN ( $\mu\text{M}$ )	DSi ( $\mu\text{M}$ )	DIP ( $\mu\text{M}$ )	DOP ( $\mu\text{M}$ )	TDP ( $\mu\text{M}$ )	TPP ( $\mu\text{M}$ )	TP ( $\mu\text{M}$ )
Surface Waters											
Lower Dafengjiang River	D1	0.90	13.10	7.73	21.73	11.75	1.59	0.91	2.50	0.22	2.72
	D2	1.01	14.60	6.43	22.04	11.27	1.31	0.51	1.82	0.25	2.07
	D3	1.01	11.40	6.15	18.56	10.47	1.07	0.10	1.17	0.32	1.49
	D4	1.13	11.08	6.20	18.41	8.82	1.47	0.22	1.69	0.31	2.00
	D5	0.80	8.88	5.15	14.83	5.85	0.94	0.47	1.41	0.19	1.60
	D6	0.85	6.60	4.68	12.13	3.96	0.82	0.59	1.41	0.24	1.65
	D7	0.78	5.85	3.30	9.93	4.29	0.22	0.38	0.60	0.22	0.82

Table 2. Cont.

Sample Locations	Site	NO <sub>2</sub> <sup>-</sup> (μM)	NO <sub>3</sub> <sup>-</sup> (μM)	NH <sub>4</sub> <sup>+</sup> (μM)	DIN (μM)	DSi (μM)	DIP (μM)	DOP (μM)	TDP (μM)	TPP (μM)	TP (μM)
Qinzhou Bay	D8	0.53	3.10	0.70	4.33	1.78	0.02	1.02	1.04	0.19	1.23
	D9	0.30	2.70	0.48	3.48	1.34	0.03	0.83	0.86	0.31	1.17
	D10	0.63	3.00	0.63	4.26	1.65	0.05	0.18	0.23	0.21	0.44
	D11	0.13	1.28	1.05	2.46	1.04	0.02	0.14	0.16	0.24	0.40
	D12	0.05	0.60	0.25	0.90	0.75	0.01	0.10	0.11	0.24	0.35
	D13	0.05	1.33	0.40	1.78	0.71	0.01	0.28	0.29	0.10	0.39
Bottom Waters											
Lower Dafengjiang River	D1	1.23	12.58	7.53	21.34	8.87	1.00	1.33	2.33	0.15	2.48
	D2	1.35	11.55	6.80	19.70	10.85	1.21	0.69	1.90	0.17	2.07
	D3	0.91	9.05	5.68	15.64	7.69	0.92	1.04	1.96	0.23	2.19
	D4	0.91	9.15	5.10	15.16	6.89	0.54	0.47	1.01	0.26	1.27
	D5	0.63	7.60	4.05	12.28	6.37	0.76	0.37	1.13	0.20	1.33
	D6	0.85	6.75	3.40	11.00	3.82	0.55	1.31	1.86	0.19	2.05
	D7	0.50	4.58	1.25	6.33	3.82	0.21	0.35	0.56	0.23	0.79
Qinzhou Bay	D8	0.58	2.88	1.30	4.76	1.27	0.02	0.66	0.68	0.17	0.85
	D9	0.58	2.78	1.58	4.94	1.11	0.02	0.89	0.91	0.27	1.18
	D10	0.58	4.73	0.50	5.81	2.41	0.04	0.50	0.54	0.24	0.78
	D11	0.45	1.28	0.63	2.36	0.90	0.02	0.20	0.22	0.21	0.43
	D12	0.48	2.55	0.15	3.18	0.61	0.02	0.50	0.52	0.26	0.78
	D13	0.10	0.78	0.68	1.56	1.04	0.01	0.29	0.30	0.04	0.34

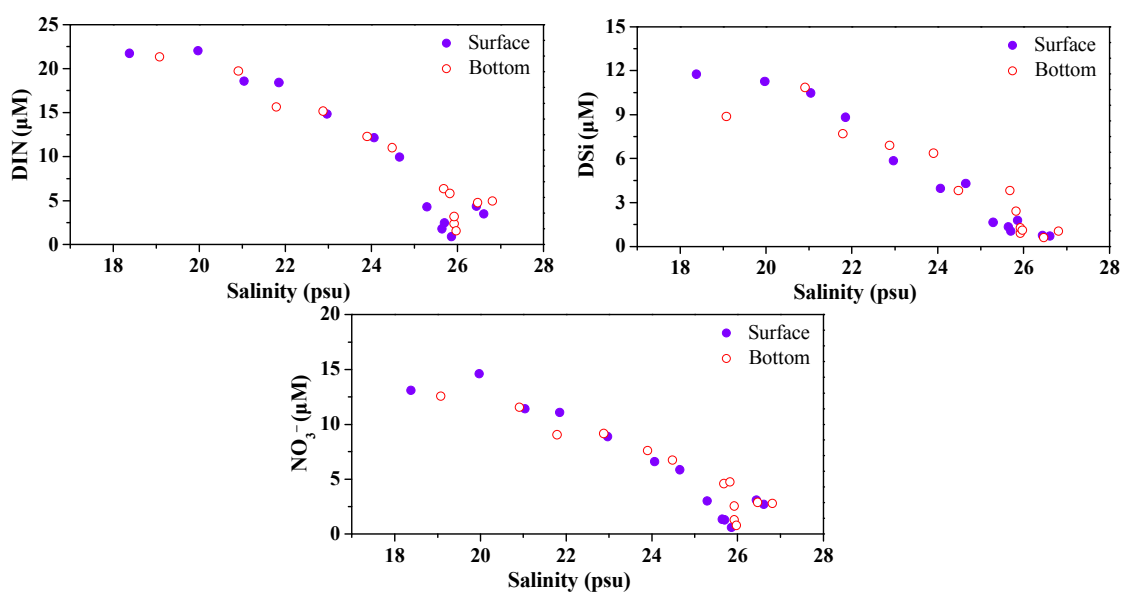
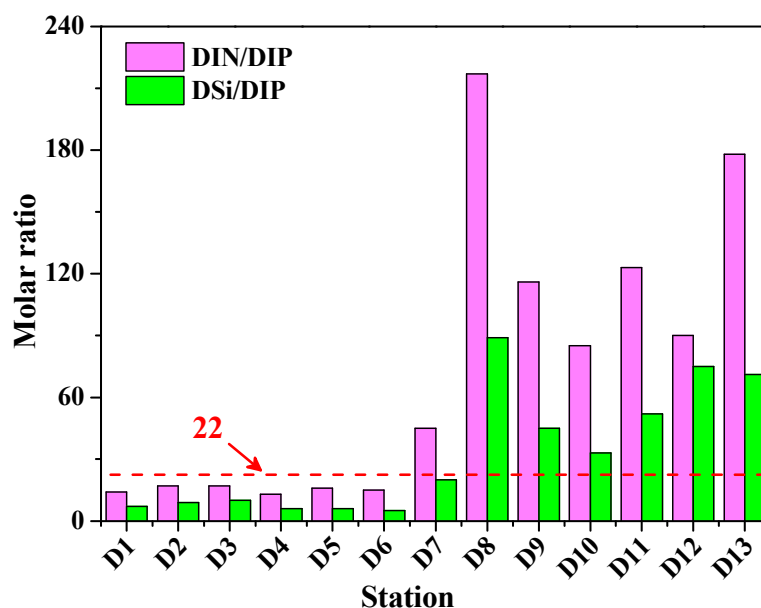


Figure 3. Spatial variations of NO<sub>3</sub><sup>-</sup>, DIN, and DSi with salinity in surface and bottom waters of the Dafengjiang River estuary.

Table 3. The relationship of DIN, DSi, DIP, and TDP vs. salinity both in surface and bottom waters of the Dafengjiang River estuary.

Water Samples	Relational Expression	R <sup>2</sup>
Surface	y = -2.8938 + 79.036 (DIN vs. salinity)	0.92
	y = -1.5725 + 42.310 (DSi vs. salinity)	0.96
	y = -0.2233 + 5.8797 (DIP vs. salinity)	0.88
	y = -0.2453 + 6.8431 (TDP vs. salinity)	0.76
Bottom	y = -2.7111 + 75.367 (DIN vs. salinity)	0.95
	y = -1.3422 + 36.869 (DSi vs. salinity)	0.86
	y = -0.1698 + 4.5330 (DIP vs. salinity)	0.85
	y = -0.2600 + 7.3839 (TDP vs. salinity)	0.77



**Figure 4.** Distributions of nutrient molar ratios in surface waters of the Dafengjiang River estuary. Ambient molar ratios of DIN/DIP and DSi/DIP > 22 indicate stoichiometric (potential) P limitation for phytoplankton growth [51].

### 3.3. Abundance and Variations in Different P Species

The concentrations of different P species both in the dissolved and particulate phases for the surface and bottom waters in the lower Dafengjiang River and Qinzhou bay are presented in Table 2. DIP concentrations (average,  $0.58 \pm 0.63 \mu\text{M}$ ) in the surface water generally decreased from  $1.59 \mu\text{M}$  at the river end-member station D1 to  $0.01 \mu\text{M}$  at the open waters station D13, where salinity was the highest (Figure 5, Table 1). Similarly, concentrations of DIP in the bottom water were also variable and generally decreased from  $1.21$  to  $0.01 \mu\text{M}$  (average,  $0.41 \pm 0.44 \mu\text{M}$ ) (Figure 5). These data suggest a strong riverine DIP source, although there seemed to be a little regeneration during early mixing, as indicated by the significant relationship between DIP and salinity both in the surface and bottom waters (Table 3). In the surface waters, concentrations of DOP were generally low compared to DIP in the lower riverine regions and higher than DIP in the bay (Figure 5); the concentration range was between  $0.10$  and  $1.02 \mu\text{M}$  (average,  $0.44 \pm 0.32 \mu\text{M}$ ). In the bottom water, concentrations of DOP were generally higher than DIP, varying from  $0.20$  to  $1.33 \mu\text{M}$  (average,  $0.66 \pm 0.37 \mu\text{M}$ ). The discrepancies in the concentrations of DIP and DOP between the surface and bottom waters at each sampling site were generally small (Table 2, Figure 5), showing a fairly mixed water column in the study area.

In the dissolved phase, the contribution of DOP to TDP pool in surface water was between 2% and 91% (average,  $59\% \pm 34\%$ ), while DIP was between 9% and 98% (average,  $41\% \pm 34\%$ ). In bottom water,  $72\% \pm 25\%$  of the TDP was composed of DOP, whereas DIP accounted for  $28\% \pm 25\%$  of TDP (Figure 5). As expected, DOP was the main dissolved P species in the water column, with the exception in the surface water samples at the lower salinity ( $S < 24$ ) stations (Figure 5). DIP was the dominant dissolved P species in the lower river water column, comprising  $58\% \pm 18\%$  of the TDP, whereas DOP became predominant (>90% on average) in the open coastal waters, suggesting an enhanced transformation between P species and a rapid shift in P source and biogeochemical cycling across the river–sea interface. The areas with higher ratios of DOP/TDP were also consistent with the areas having elevated Chl-*a* levels in the Qinzhou Bay (Figures 2 and 5). Therefore, riverine inputs and biological production likely have a significant influence on the dynamic distribution of different dissolved P species in the study area.

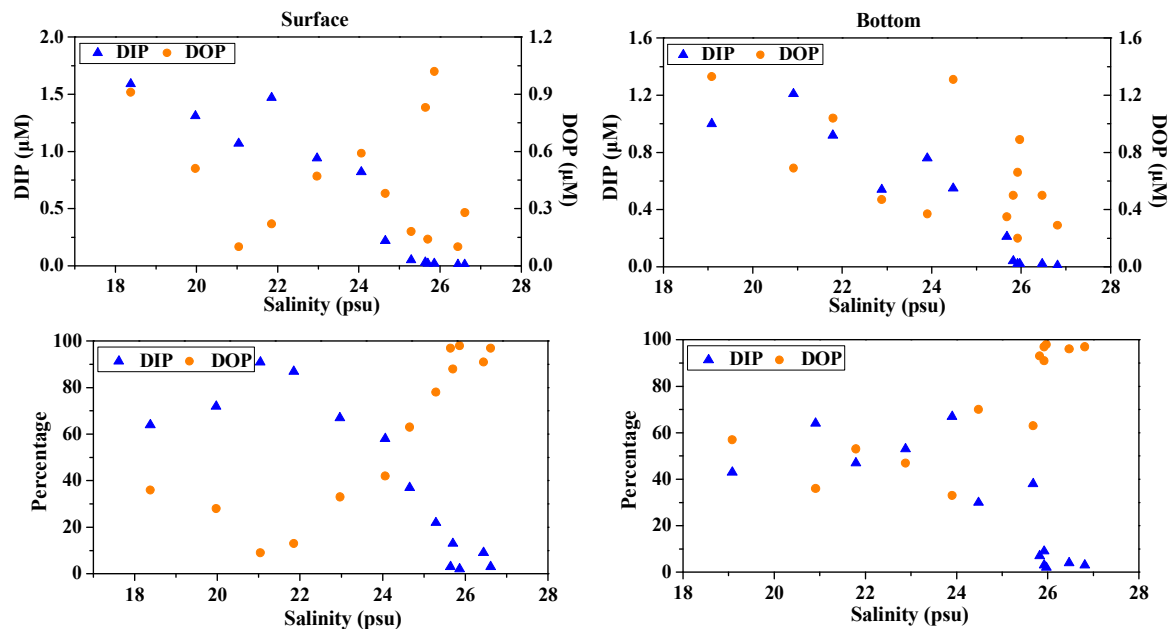


**Figure 5.** Variations in concentration and percentage of DIP and DOP with salinity in surface water (surface, left panels) and bottom waters (bottom, right panels) of the Dafengjiang River estuary.

Surface water TDP concentrations were highly variable, ranging from 0.11  $\mu\text{M}$  to 2.50  $\mu\text{M}$  (average,  $1.02 \pm 0.74 \mu\text{M}$ ), while TDP in the bottom water was slightly higher than the surface and varied between 0.22  $\mu\text{M}$  and 2.33  $\mu\text{M}$  (average,  $1.07 \pm 0.71 \mu\text{M}$ ) (Table 2). TDP concentrations decreased with increasing salinity both in the surface and bottom waters (Figure 6) and showed a predominant river influence. This was manifested by the significant relationship between TDP and salinity (Table 3). Concentrations of TPP were generally low and less variable relative to TDP. TPP concentrations ranged from 0.10  $\mu\text{M}$  to 0.32  $\mu\text{M}$  (average,  $0.23 \pm 0.06 \mu\text{M}$ ) in the surface water and 0.04  $\mu\text{M}$  to 0.27  $\mu\text{M}$  (average,  $0.20 \pm 0.06 \mu\text{M}$ ) in the bottom water.

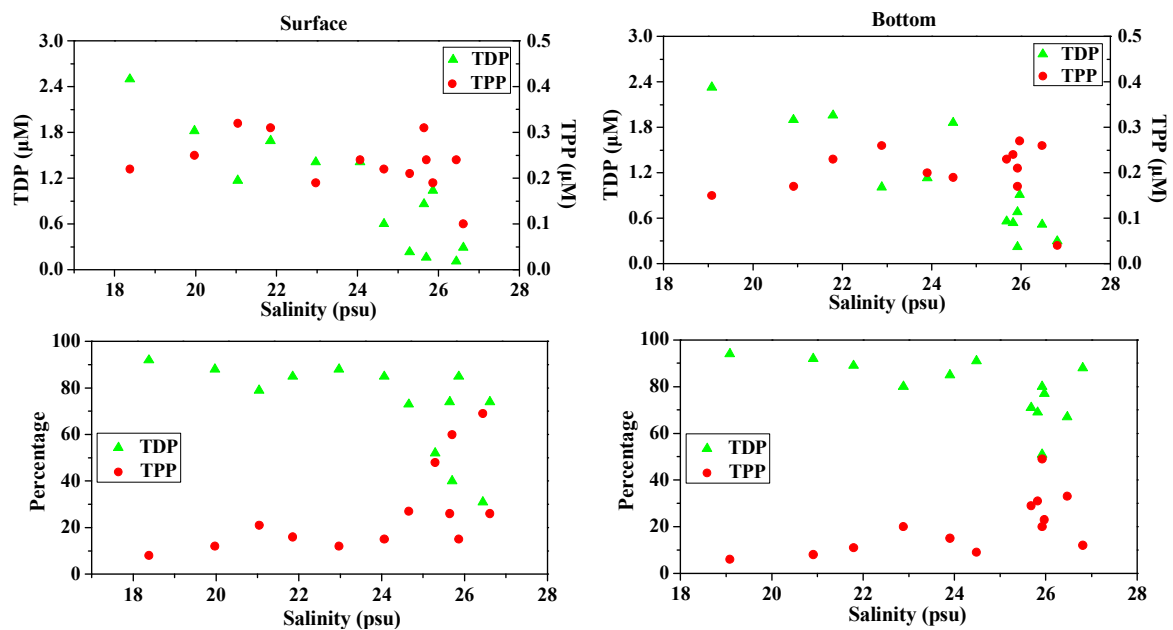


**Figure 6.** Variations in concentration and percentage of TDP and TPP with salinity in surface water (surface, left panels) and bottom waters (bottom, right panels) of the Dafengjiang River estuary.

Considering both dissolved and particulate P phases, dissolved P was the predominant phase in the total P pool in the study area, ranging from 31% to 92% (average,  $73\% \pm 19\%$ ) in surface waters, and 51% to 94% (average,  $80\% \pm 12\%$ ) in bottom waters (Figure 6), implying that riverine export of P was mainly in the dissolved phase, as indicated by the significant relationship between TDP vs salinity both in surface and bottom waters (Table 3). As the salinity increased above 25 psu, the increasing TPP/TP ratios in the water column were comparable to the decreasing in TDP/TP ratios (Figure 6), suggesting a transformation of P between dissolved and particulate phases in the coastal waters.

### 3.4. Partitioning of P between Dissolved and Particulate Phases

As shown in Figure 7, the percentage contribution of DIP to TDP pool decreased from the surface to bottom water, whereas the percentage composition of DOP was higher in the bottom water than surface water. The concentrations of TPP were generally lower than TDP in the water column (Table 2, Figure 6). On average, TPP accounted for  $24\% \pm 16\%$  of the total P pool in the study area (Table 2). The percentage of TPP in the TP pool decreased from  $27\% \pm 19\%$  in the surface water to  $20\% \pm 12\%$  in bottom water (Figure 7). Interestingly, the percentage of DIP in TP decreased dramatically from  $50\% \pm 16\%$  in the lower Dafengjiang River to  $4\% \pm 2\%$  in the Qinzhou Bay (Table 2, Figure 7), likely due to the uptake by phytoplankton and tidal dilution of coastal waters. This is indicated by the high water temperature and salinity and the elevated Chl-*a* levels in the coastal water column (Figure 2a–d,g,h). On the contrary, the percentage contribution of DOP to TP increased from  $35\% \pm 15\%$  in river water to  $62\% \pm 19\%$  in coastal water (Figure 7). This suggests biological production of DOP in the coastal water, as certified by the elevated Chl-*a* levels in the coastal water column (Figure 2g,h). Similarly, the percentage of TPP in the TP pool increased from  $15\% \pm 7\%$  in lower river water to  $34\% \pm 18\%$  in coastal water (Figure 7). This shows the significance of TPP in coastal waters of the study area.

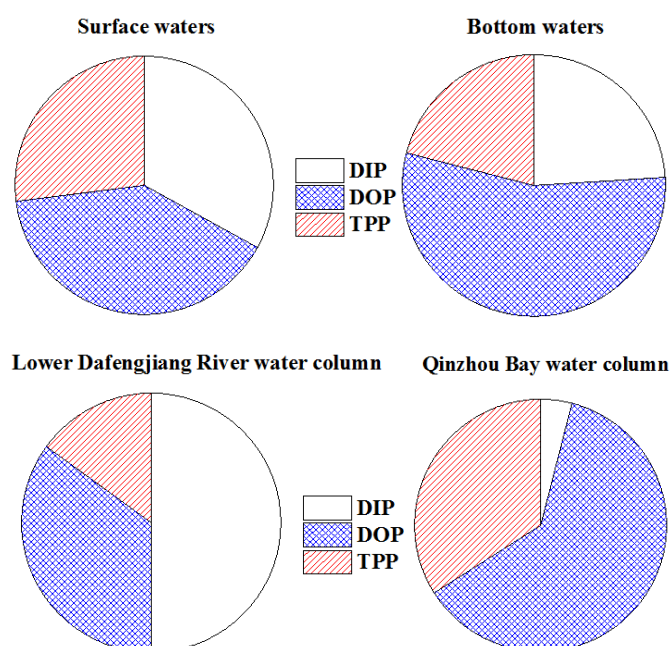


**Figure 7.** The partitioning of P among DIP, DOP, and TPP in surface waters, bottom waters, lower Dangfengjiang River water column, and Qinzhou Bay water column.

## 4. Discussion

### 4.1. Abundance and Partitioning of P Species

Compared to other rivers around the world, the average concentration of DIP ( $1.06 \pm 0.46 \mu\text{M}$ ) in the lower Dafengjiang River surface water is lower than many heavily human-influenced and

eutrophic rivers, such as the Milwaukee River [6], Mississippi River [44,52], Maumee River [53], Jiulong River [8], and Scheldt estuary [54] (Table 4), but higher than those of more pristine rivers, such as the Jourdon River in Mississippi [55], Chena River in interior Alaska [56], and the Yukon River [57,58]. This reflects the fact that the lower Dafengjiang River has been somewhat disturbed by human activities. Unlike rivers that are heavily affected by anthropogenic activities and having elevated DIP/TDP ratios (up to 0.9), such as the Maumee River and the Mississippi River, which have impacts on the development of hypoxia in Lake Erie and the northern Gulf of Mexico, respectively (Table 4), the lower Dafengjiang River had an intermediate DIP/TDP ratio (average,  $0.68 \pm 0.18$ ) and DOP/TDP (average,  $0.32 \pm 0.18$ ) during the study period. The DIP/TDP ratios recorded in the lower Dafengjiang River are also higher than those of pristine rivers, such as the Jourdon River in Mississippi (Table 4). Compared with many other rivers where TPP was dominant in the TP pool (e.g., Mississippi River, Maumee River, Jourdon River, Chena River, and Jiulong River (Table 4)), P exported from the lower Dafengjiang River to Qinzhou Bay was predominantly in the dissolved form (Figure 7). Within the total P pool, the TPP abundance was lower than TDP in the lower Dafengjiang River and was consistent with the previous observations in the Milwaukee River, where TDP was the predominant P species of the total P pool [6] but distinct from observations made in the other rivers (Table 4).

**Table 4.** Comparisons of the abundance of DIP, DOP, and TPP and their partitioning in TP pool between different rivers. All values are for surface waters. Values in parentheses denote the averaged concentrations and their standard deviations.

Study Area	DIP ( $\mu\text{M}$ )	DOP ( $\mu\text{M}$ )	TPP ( $\mu\text{M}$ )	DIP/TP (%)	DOP/TP (%)	TPP/TP (%)	Reference
Fox River	0.68–0.98 ( $0.83 \pm 0.22$ )	0.52–0.68 ( $0.60 \pm 0.11$ )	1.97	24	18	58	[59]
Milwaukee River	0.69–3.05 ( $1.81 \pm 1.19$ )	0.11–0.91 ( $0.54 \pm 0.38$ )	1.38	47	16	37	[6]
Mississippi River	2.07–4.20 ( $2.89 \pm 1.15$ )	0.24–0.45 ( $0.35 \pm 0.15$ )	5.26	34	4	62	[44,52]
Maumee Rive	2.74	0.07	14.26	16	0.3	83.7	[53]
Jourdon River	0.03	0.16	0.97	3	14	83	[55]
Chena River	0.03–0.30	0.06 $\pm$ 0.06	0.6	19	7	74	[56]
Jiulong River	2.14	0.55	5.11	27	7	66	[8]
Scheldt estuary	3.3	0.7	5.2	36	8	56	[54]
Dafengjiang River	0.22–1.59 ( $1.06 \pm 0.46$ )	0.10–0.91 ( $0.45 \pm 0.26$ )	0.22	58	27	15	This study

Accompanying the variation in the concentrations of different P species, the partitioning of P between the inorganic and organic phases of the TDP pool also changed significantly across the river–sea interface (Figure 7). The elevated percentage of DIP in surface waters, which was found where the percentage of TPP was relatively higher, was largely as a result of particulate P regeneration (e.g., through bacterial processes) and the subsequent release of DIP [6,60]. The higher DOP in bottom waters may have been derived from the effects of benthic processes, including sediment resuspension and possible release of DOP from surface sediments into the overlying water column [61]. Additionally, it shifted from a DIP-dominated and human-influenced river setting to DOP-dominated and P-limiting conditions in the coastal waters. Evidently, the TDP pool was composed mainly of DIP in the lower Dafengjiang River and mainly influenced by river input. Abundance of DOP was observed in coastal waters (Figure 5), which matched the elevated Chl-*a* level (Figure 2). This showed the influence of biological in situ production and biomass on DOP under a DIP-limiting setting [62]. In contrast, low abundance of DIP in the coastal water column was largely as a result of related biological processes including DIP uptake by phytoplankton such as *Phaeocystis globosa* [63]. In addition to biological processes, abundance of DOP may have also been enhanced by physicochemical processes including adsorption/desorption and coagulation/sedimentation. The river-derived P could be directly transported to the sediment and may be converted into organic phase in coastal waters [6]. However, further studies would be essential for better understanding of the specific biogeochemical processes affecting P cycling across the river–sea interface.

#### 4.2. Factors Controlling and Source of the Different P Species

Correlation analysis and factor analysis were performed on the P species and all environmental parameters in order to confirm the data structure and identify the factors controlling the dynamics of P species in the study area. With the exception of DOP, all dissolved nutrients showed a significantly negative correlation with salinity ( $p < 0.01$ ) and were negatively correlated with DO and pH ( $p < 0.01$ ) (Table 5). Again, Chl-*a* showed a significantly negative correlation with DOP, TDP, and TP ( $p < 0.05$ ), suggesting that P is the controlling factor for the phytoplankton abundance in the water column, among other nutrients, in the study area.

**Table 5.** Pearson correlation matrix for the P species and physicochemical parameters in the water column of the Dafengjiang River estuary.

	T	S	pH	DO	DIN	DSi	Chl- <i>a</i>	DIP	DOP	TDP	TPP	TP
T												
S	0.343											
pH	0.384	0.944 <sup>a</sup>										
DO	0.429 <sup>b</sup>	0.674 <sup>a</sup>	0.815 <sup>a</sup>									
DIN	−0.445 <sup>b</sup>	−0.967 <sup>a</sup>	−0.971 <sup>a</sup>	−0.771 <sup>a</sup>								
DSi	−0.402 <sup>b</sup>	−0.960 <sup>a</sup>	−0.972 <sup>a</sup>	−0.754 <sup>a</sup>	0.974 <sup>a</sup>							
Chl- <i>a</i>	0.072	0.342	0.216	0.144	−0.318	−0.299						
DIP	−0.356	−0.931 <sup>a</sup>	−0.956 <sup>a</sup>	−0.770 <sup>a</sup>	0.955 <sup>a</sup>	0.949 <sup>a</sup>	−0.253					
DOP	−0.301	−0.331	−0.227	−0.118	0.317	0.206	−0.435 <sup>b</sup>	0.214				
TDP	−0.424 <sup>b</sup>	−0.877 <sup>a</sup>	−0.843 <sup>a</sup>	−0.646 <sup>a</sup>	0.888 <sup>a</sup>	0.827 <sup>a</sup>	−0.413 <sup>b</sup>	0.870 <sup>a</sup>	0.668 <sup>a</sup>			
TPP	−0.003	−0.176	−0.145	0.056	0.205	0.206	−0.168	0.202	−0.118	0.094		
TP	−0.419 <sup>b</sup>	−0.882 <sup>a</sup>	−0.846 <sup>a</sup>	−0.634 <sup>a</sup>	0.895 <sup>a</sup>	0.835 <sup>a</sup>	−0.422 <sup>b</sup>	0.877 <sup>a</sup>	0.650 <sup>a</sup>	0.996 <sup>a</sup>	0.179	

<sup>a</sup> Correlation is significant at the 0.01 level (two-tailed).  $n = 26$ . <sup>b</sup> Correlation is significant at the 0.05 level (two-tailed).  $n = 26$ .

In order to identify the sources of P species in the water column, factor analysis was applied by considering various variables after varimax rotation. Although the water column is well mixed, the spatial differences among various P species and other environmental parameters are significant (ANOVA,  $p < 0.05$ ) in the column in addition to water temperature. Thus, the variables included P species (DIP, DOP, TDP, TPP, and TP) and other physicochemical and biological parameters, i.e., S, pH, DO, DIN, DSi, and Chl-*a*. The examination of the cumulative loading displayed a total variance of 85.25% for the first three components extracted based on the eigenvalues  $> 1$ . The first factor (F1) accounted for 63.39% of the total variance and revealed a very strong positive loading for DIP, TDP, TP, DIN, and DSi and strong negative loading for salinity, pH, and DO (Table 6). Furthermore, the results of the correlation analysis show that all dissolved inorganic nutrients have a significant negative correlation with salinity, pH, and DO (Table 5). This suggests that the nutrient concentrations increased with the dilution of salinity, the decline of pH, and the depletion of oxygen and vice-versa. The freshwater runoff from the upstream sewage discharge and the dilution of tides ultimately affect the dissolved inorganic nutrients' abundance and distribution. Thus, factor 1 can be considered a "physical factor". The second factor (F2) accounted for 12.14% of the total variance, with strong positive loading for DOP and negative loading for Chl-*a*. In accordance with the loading of F2, the correlation analysis displayed an inverse relation between DOP and Chl-*a* (Table 5), which specifies that the Chl-*a* level increased with decreasing DOP concentration and vice-versa. Phytoplankton utilizes DOP as a P source in order to maintain its growth when DIP is deficient [15,64]. The concentration range (0.01–0.05  $\mu\text{M}$ ) of DIP in the coastal region was lower than the threshold value (0.1  $\mu\text{M}$ ) required for phytoplankton growth [51] during the study period. Consequently, DOP played a significant role by complementing DIP limitation for phytoplankton growth, i.e., as an alternative P source in the coastal region, as depicted by high Chl-*a* levels in the water column (Figure 2). Therefore, F2 can be termed a "biological factor". Finally, the third factor (F3) accounted for 9.72% of the total variance, with strong positive loading for TPP. This may be due to algae picking up dissolved P and forming it into particulate [8], which is different from dissolved inorganic nutrients. Thus, this factor can also be

considered a “biological factor”. The results of the factor analysis indicated that the dynamics of P species in the water column of the study area were controlled both by physical and biological processes.

**Table 6.** Rotated varimax factor analysis of the various P species and environmental parameters in the water column of the Dafengjiang River estuary.

	F1	F2	F3
S	−0.951	−0.402	−0.083
pH	−0.983	−0.250	−0.008
DO	−0.831	0.079	0.233
DIN	0.986	0.372	0.047
DSi	0.971	0.283	0.090
Chl- <i>a</i>	−0.258	−0.758	−0.293
DIP	0.971	0.283	0.079
DOP	0.301	0.902	−0.302
TDP	0.892	0.671	−0.092
TPP	0.147	0.079	0.863
TP	0.894	0.670	−0.017
Eigenvalue	7.607	1.456	1.167
% of variance	63.39	12.14	9.720
Cumulative% of variance	63.39	75.53	85.25

Notes: Extraction method: PCA. Rotation method: Varimax with Kaiser Normalization.

#### 4.3. Effect of the Dafengjiang River Discharge on P Dynamics

Temporal variations in the river discharge had an important impact on both the hydrodynamic conditions and concentrations of nutrients [7]. During the early winter in December 2017, the thorough vertical mixing of the water column resulted in no significant variations of TPP concentrations between the surface and bottom waters (Figure 6). In addition, during the investigation period in the dry season, only approximately 20% of the river discharge occurred from October to March [34]. As a result, the TDP and TPP concentrations were low ( $1.05 \mu\text{M}$  and  $0.19 \mu\text{M}$ , on average) in the water column, respectively, especially TPP. The TPP levels in the DRE were low compared to some tropical estuaries that are significantly affected by anthropogenic activities, such as the Pearl River estuary [7], the Wenchang River, and Wenjiao River in Hainan Island in China [65]. During the study period, contents of Chl-*a* in the water column were lower (average,  $3.74 \pm 1.26 \mu\text{g L}^{-1}$ ) in the riverine regions and elevated (average,  $4.69 \pm 1.59 \mu\text{g L}^{-1}$ ) in the coastal region (Table 1). Senthikumar et al. (2008) had reported Chl-*a* concentrations (average,  $5.35 \pm 1.5 \mu\text{g L}^{-1}$ ) during the dry season at the southeast coast of India [66], which was similar to the DIP concentrations in the lower Dafengjiang River. Chl-*a* is often used as the most reliable indicator of phytoplankton biomass. This suggests that phytoplankton growth may be affected by light limitation, since strong vertical mixing causes sediment resuspension and, as a result, reduces light intensity in the water column for primary production [59]. The same results were found in the tropical northern Gulf of Carpentaria in winter [67]. Therefore, light limitation triggered by strong vertical mixing might be responsible for the lower Ch-*a* level in the lower riverine regions despite elevated nutrient levels. However, in the coastal area, open waters exchange enhanced light levels in the water column and facilitated phytoplankton growth, which resulted in elevated Chl-*a* level (Figure 2g,h). Thus, phytoplankton uptake might lead to DIP depletion.

In the present study, the two-end-member mixing model was applied to differentiate the physically caused variations in the DIP concentrations from the biological uptake in the study area. The freshwater end-member was based on the surface water salinity (18.38) and DIP concentration ( $1.59 \mu\text{M}$ ) at station D1. The seawater end-member was obtained by surface water salinity (26.61) and DIP concentration ( $0.01 \mu\text{M}$ ) at station D13. The removal and deviation from the theoretical mixing line might be ascribed to the influence of the river discharge [7,68]. As shown in Figure 8a and the deviation from the theoretical mixing line, positive deviations were observed at most stations in the coastal area, while negative deviations appeared at estuarine mixing stations with salinity between 22 psu and

24 psu (Figure 8b). This indicates that DIP depletion was caused by biological uptake in the coastal region while DIP addition, which occurred in the estuarine mixing region, was likely due to the release from particulate P or sediment caused by strong vertical mixing. Based on the two-end-member mixing model, the biological uptake resulted in a DIP reduction by a factor of  $0.12 \pm 0.08 \mu\text{M}$  at the coastal surface water. This was responsible for a rapid increase in the relative contribution of DOP to TDP (Figure 5) and considerably high molar ratios of DIN/DIP in the high salinity waters ( $S > 24$ ) (Figure 4). According to the Redfield ratio ( $C:P = 106:1 \text{ mol mol}^{-1}$ ), the carbon uptake by phytoplankton at the surface was estimated to be  $153 \mu\text{g C L}^{-1}$ . In comparison, the replenishment of DIP from particulate P or sediment led to an increase ( $0.19 \pm 0.22 \mu\text{M}$ ) in DIP in the estuarine mixing region.

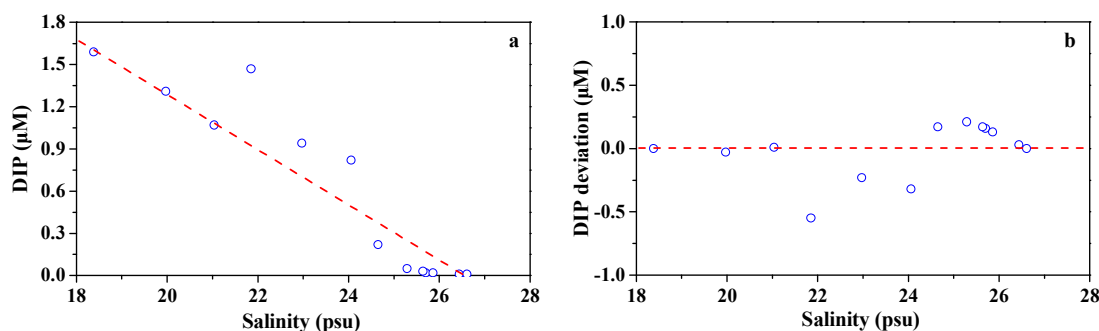


**Figure 8.** The DIP concentrations versus salinity in the surface waters from the lower Dafengjiang River to Qinzhou Bay. The dashed line denotes the theoretical mixing line between freshwater and seawater end members in the plot of DIP vs. salinity. The deviation of DIP represents the difference between the DIP concentrations forecasted based on the two-end-member mixing model and the ambient DIP concentrations. The dashed line denotes no deviation in DIP in the plot of DIP deviation vs. salinity. The positive and negative deviations indicate DIP drawdown by biological uptake and DIP addition, respectively.

## 5. Conclusions

The abundance, distribution, and phase partitioning of dissolved and particulate P in the surface and bottom water were systematically examined for the first time across the river–sea interface from the lower Dafengjiang River to the open Beibu Gulf. Concentrations of dissolved inorganic nitrogen, silicate, and phosphate decreased from the lower Dafengjiang River to coastal waters, but the chemical speciation and partitioning of P changed considerably from river to sea waters. TDP was predominant in the total P pool, which was consistent with those observed in the Milwaukee River but was distinct from other global rivers. Within the total P pool, DIP was the dominant species in the surface waters, showing particle P regeneration and release into the DIP. In contrast, DOP that dominated in bottom waters may be derived from the effects of benthic processes. DIP became predominant in the lower river water column and showed a predominant river influence, while DOP that dominated in the coastal region was largely the result of physicochemical and biological processes. Correlation and factor analysis further indicated that the dynamics of P species in the water column were mainly controlled by both physical and biological processes. In the surface waters, the depletion of DIP concentrations were caused by biological uptake in the coastal region, whereas the addition of DIP that occurred in the estuarine mixing region was likely due to the replenishment of DIP from the release of particulate P or sediment caused by strong vertical mixing. Different P species could play a significant role in the biogeochemical cycling of P in the water column. Therefore, knowledge of the detailed chemical and phase speciation of P should contribute to better understanding of the dynamic cycling of P in the tropical estuarine and coastal environments.

**Author Contributions:** B.Y. and D.-L.L. designed the study; Z.-J.K. performed the field sampling and sample pretreatment; S.F.D. carried out English editing on the article; Z.-M.N. analyzed the data; W.-L.L. performed the sample measurements; Q.-P.Z. collected the data; B.Y. wrote and revised the article.

**Funding:** This work was supported by grants from the National Natural Science Foundation of China (Nos. 41706083, 41576083 and 41466001), Natural Science Foundation of Guangxi (Nos. 2017GXNSFBA198135 and 2016GXNSFBA380108), Scientific Research Fund of Guangxi Education Department (No. KY2016YB494), the project of Qinzhou Science Research and Technology Development (No. 20164403), the project of Guangxi Key Laboratory of Marine Disaster in the Beibu Gulf (No. 2017TS10), the Guangxi “Marine Ecological Environment” Academician Workstation Capacity Building (No. Gui Science AD17129046), the Science and Technology Major Project of Guangxi (No. AA17204095-10), and the Distinguished Experts Programme of Guangxi Province.

**Acknowledgments:** We are sincerely grateful to colleagues from the marine biogeochemistry laboratory for providing support and help. We would also like to thank the two anonymous reviewers for their constructive comments which improved the manuscript.

**Conflicts of Interest:** The authors declare no conflict of interest.

## Abbreviations

P	Phosphorus
TP	Total phosphorus
TDP	Total dissolved phosphorus
DIP	Dissolved inorganic phosphorus
DOP	Dissolved organic phosphorus
TPP	Total particulate phosphorus
DSi	Dissolved silicate
PCA	Principal component analysis
DRE	Dafengjiang River estuary
DIN	Dissolved inorganic nitrogen
NO <sub>3</sub> <sup>−</sup>	Nitrate
NO <sub>2</sub> <sup>−</sup>	Nitrite
NH <sub>4</sub> <sup>+</sup>	Ammonium
T	Temperature
S	Salinity
DO	Dissolved oxygen
Chl- <i>a</i>	Chlorophyll <i>a</i>

## References

- Slomp, C.P. Phosphorus cycling in the estuarine and coastal zones: Sources, sinks, and transformations. In *Treatise on Estuarine and Coastal Science*; Wolanski, E., McLusky, D.S., Eds.; Academic Press: Waltham, MA, USA, 2011; Volume 5, pp. 201–229, ISBN 9780080878850.
- Yang, B.; Song, G.D.; Liu, S.M.; Jin, J. Phosphorus recycling and burial in core sediments of the East China Sea. *Mar. Chem.* **2017**, *192*, 59–72. [[CrossRef](#)]
- Yang, B.; Liu, S.M.; Zhang, G.L. Geochemical characteristics of phosphorus in surface sediments from the continental shelf region of the northern South China Sea. *Mar. Chem.* **2018**, *198*, 44–55. [[CrossRef](#)]
- Yang, B.; Liu, S.M.; Wu, Y.; Zhang, J. Phosphorus speciation and availability in sediments off the eastern coast of Hainan Island, South China Sea. *Cont. Shelf Res.* **2016**, *118*, 111–127. [[CrossRef](#)]
- Bastami, K.D.; Neyestani, M.R.; Raeisi, H.; Shafeian, E.; Baniamam, M.; Shirzadi, A.; Esmailzadeh, M.; Mozaffari, S.; Shahrokhi, B. Bioavailability and geochemical speciation of phosphorus in surface sediments of the Southern Caspian Sea. *Mar. Pollut. Bull.* **2018**, *126*, 51–57. [[CrossRef](#)] [[PubMed](#)]
- Lin, P.; Guo, L.D. Dynamic changes in the abundance and chemical speciation of dissolved and particulate phosphorus across the river-lake interface in southwest Lake Michigan. *Limnol. Oceanogr.* **2016**, *61*, 771–789. [[CrossRef](#)]
- Li, R.H.; Xu, J.; Li, X.F.; Shi, Z.; Harrison, P.J. Spatiotemporal variability in phosphorus species in the Pearl River Estuary: Influence of the river discharge. *Sci. Rep.* **2017**, *7*, 13649. [[CrossRef](#)] [[PubMed](#)]

8. Lin, P.; Guo, L.D.; Chen, M.; Cai, Y.H. Distribution, partitioning and mixing behavior of phosphorus species in the Jiulong River estuary. *Mar. Chem.* **2013**, *157*, 93–105. [[CrossRef](#)]
9. Lim, J.H.; Lee, C.W.; Bong, C.W.; Affendi, Y.A.; Hii, Y.S.; Kudo, I. Distributions of particulate and dissolved phosphorus in aquatic habitats of Peninsular Malaysia. *Mar. Pollut. Bull.* **2018**, *128*, 415–427. [[CrossRef](#)] [[PubMed](#)]
10. Hecky, R.E.; Kilham, P. Nutrient limitation of phytoplankton in freshwater and marine environments: A review of recent evidence on the effects of enrichment. *Limnol. Oceanogr.* **1988**, *33*, 796–822. [[CrossRef](#)]
11. Vilmin, L.; Aissa-Grouz, N.; Garnier, J.; Billen, G.; Mouchel, J.M.; Poulin, M.; Flipo, N. Impact of hydro-sedimentary processes on the dynamics of soluble reactive phosphorus in the Seine River. *Biogeochemistry* **2015**, *122*, 229–251. [[CrossRef](#)]
12. Boyer, L.A.; Plath, K.; Zeitlinger, J.; Brambrink, T.; Medeiros, L.A.; Lee, T.I.; Levine, S.S.; Wernig, M.; Tajonar, A.; Ray, M.K.; et al. Polycomb complexes repress developmental regulators in murine embryonic stem cells. *Nature* **2006**, *441*, 349–353. [[CrossRef](#)] [[PubMed](#)]
13. Huang, X.L.; Zhang, J.Z. Spatial variation in sediment-water exchange of phosphorus in Florida Bay: AMP as a model organic compound. *Environ. Sci. Technol.* **2010**, *44*, 7790–7795. [[CrossRef](#)] [[PubMed](#)]
14. Ruttenberg, K.C.; Sulak, D.J. Sorption and desorption of dissolved organic phosphorus onto iron (oxyhydr) oxides in seawater. *Geochim. Cosmochim. Acta* **2011**, *75*, 4095–4112. [[CrossRef](#)]
15. Nausch, M.; Nausch, G. Dissolved phosphorus in the Baltic Sea—Occurrence and relevance. *J. Mar. Syst.* **2011**, *87*, 37–46. [[CrossRef](#)]
16. Yoshimura, T.; Nishioka, J.; Ogawa, H.; Kuma, K.; Saito, H.; Tsuda, A. Dissolved organic phosphorus production and decomposition during open ocean diatom blooms in the subarctic Pacific. *Mar. Chem.* **2014**, *165*, 46–54. [[CrossRef](#)]
17. Huang, B.Q.; Ou, L.J.; Wang, X.L.; Huo, W.Y.; Li, R.X.; Hong, H.S.; Zhu, M.Y.; Qi, Y.Z. Alkaline phosphatase activity of phytoplankton in East China Sea coastal waters with frequent harmful algal bloom occurrences. *Aquat. Microb. Ecol.* **2007**, *49*, 195–206. [[CrossRef](#)]
18. Boge, G.; Lespilette, M.; Jamet, D.; Jamet, J.L. Role of sea water DIP and DOP in controlling bulk alkaline phosphatase activity in the N. W. Mediterranean Sea (Toulon, France). *Mar. Pollut. Bull.* **2012**, *64*, 1986–1996. [[CrossRef](#)] [[PubMed](#)]
19. Suzumura, M.; Hashihama, F.; Yamada, N.; Kinouchi, S. Dissolved phosphorus pools and alkaline phosphatase activity in the euphotic zone of the western North Pacific Ocean. *Front. Microbiol.* **2012**, *3*, 99. [[CrossRef](#)] [[PubMed](#)]
20. Paytan, A.; McLaughlin, K. The oceanic phosphorus cycle. *Chem. Rev.* **2007**, *107*, 563–576. [[CrossRef](#)] [[PubMed](#)]
21. Lin, P.; Guo, L.D.; Chen, M.; Tong, J.L.; Lin, F. The distribution and chemical speciation of dissolved and particulate phosphorus in the Bering Sea and the Chukchi–Beaufort Seas. *Deep Sea Res. Part II* **2012**, *81*, 79–94. [[CrossRef](#)]
22. Conley, D.J.; Smith, W.M.; Cornwell, J.C.; Fisher, T.R. Transformation of particle-bound phosphorus at the land-sea interface. *Estuar. Coast. Shelf Sci.* **1995**, *40*, 161–176. [[CrossRef](#)]
23. Jordan, T.E.; Cornwell, J.C.; Boynton, W.R.; Anderson, J.T. Changes in phosphorus biogeochemistry along an estuarine salinity gradient: The iron conveyor belt. *Limnol. Oceanogr.* **2008**, *53*, 172–184. [[CrossRef](#)]
24. Slomp, C.P.; Van der Gaast, S.J.; Van Raaphorst, W. Phosphorus binding by poorly crystalline iron oxides in North Sea sediments. *Mar. Chem.* **1996**, *52*, 55–73. [[CrossRef](#)]
25. Lin, P.; Klump, J.V.; Guo, L.D. Variations in chemical speciation and reactivity of phosphorus between suspended-particles and surface-sediments in seasonal hypoxia-influenced Green Bay. *J. Great Lakes Res.* **2018**. [[CrossRef](#)]
26. Meng, J.; Yao, P.; Yu, Z.G.; Bianchi, T.S.; Zhao, B.; Pan, H.H.; Li, D. Speciation, bioavailability and preservation of phosphorus in surface sediments of the Changjiang Estuary and adjacent East China Sea inner shelf. *Estuar. Coast. Shelf Sci.* **2014**, *144*, 27–38. [[CrossRef](#)]
27. Tang, D.L.; Kester, D.R.; Ni, I.H.; Qi, Y.Z.; Kawamura, H. In situ and satellite observations of a harmful algal bloom and water condition at the Pearl River estuary in late autumn 1998. *Harmful Algae* **2003**, *2*, 89–99. [[CrossRef](#)]
28. Chai, C.; Yu, Z.M.; Song, X.X.; Cao, X.H. The status and characteristics of eutrophication in the Yangtze River (Changjiang) Estuary and the adjacent East China Sea, China. *Hydrobiologia* **2006**, *563*, 313–328. [[CrossRef](#)]

29. Zhu, Z.Y.; Zhang, J.; Wu, Y.; Zhang, Y.Y.; Lin, J.; Liu, S.M. Hypoxia off the Changjiang (Yangtze River) Estuary: oxygen depletion and organic matter decomposition. *Mar. Chem.* **2011**, *125*, 108–116. [[CrossRef](#)]
30. Yang, B.; Fang, H.Y.; Zhong, Q.P.; Zhang, C.X.; Li, S.P. Distribution characteristics of nutrients and eutrophication assessment in summer in Qinzhou Bay. *Mar. Sci. Bull.* **2012**, *31*, 640–645. (In Chinese)
31. Lai, J.X.; Jiang, F.J.; Ke, K.; Xu, M.B.; Lei, F.; Chen, B. Nutrients distribution and trophic status assessment in the northern Beibu Gulf, China. *Chin. J. Oceanol. Limnol.* **2014**, *32*, 1128–1144. [[CrossRef](#)]
32. Yang, B.; Zhong, Q.P.; Zhang, C.X.; Lu, D.L.; Liang, Y.R.; Li, S.P. Spatio-temporal variations of chlorophyll *a* and primary productivity and its influence factors in Qinzhou Bay. *Acta Sci. Circums.* **2015**, *35*, 1333–1340. (In Chinese)
33. Li, P.Y.; Xue, R.; Wang, Y.H.; Zhang, R.J.; Zhang, G. Influence of anthropogenic activities on PAHs in sediments in a significant gulf of low-latitude developing regions, the Beibu Gulf, South China Sea: distribution, sources, inventory and probability risk. *Mar. Pollut. Bull.* **2015**, *90*, 218–226. [[CrossRef](#)] [[PubMed](#)]
34. Luo, Y.F.; Huang, H.J.; Yan, L.W.; Bi, H.B.; Zhang, Z.H. Distribution and diffusion of suspended matters based on remote sensing in the Dafengjiang Estuary. *Trans. Oceanol. Limnol.* **2005**, *27*, 14–20. (In Chinese)
35. Committee of Annals of Chinese Estuaries. *Annals of Chinese Estuaries*; Ocean Press: Beijing, China, 1998; Volume 14. (In Chinese)
36. Xu, S.Q.; Li, J.M.; Lu, S.B.; Zhong, Q.P.; Chen, M.E. Current situation and sustainable development of mangrove resources in the Guangxi Beibu Gulf. *Bull. Biol.* **2010**, *45*, 11–14. (In Chinese)
37. Lagos, J.E.; Jiang, J.; Sindelar, S. *Peoples Republic of China Sugar Annual 2011*; Required Report–Public Distribution CH11019; Global Agricultural Information Network (GAIN): Beijing, China, 2011.
38. Bai, J.; Gan, S. Eucalyptus plantations in China. In Reports Submitted to the Regional Expert Consultation on Eucalyptus. FAO Regional Office for Asia and the Pacific (RAP): Bangkok, Thailand, 1996.
39. Herbeck, L.S.; Sollich, M.; Unger, D.; Holmer, M.; Jennerjahn, T.C. Impact of pond aquaculture effluents on seagrass performance in NE Hainan, tropical China. *Mar. Pollut. Bull.* **2014**, *85*, 190–203. [[CrossRef](#)] [[PubMed](#)]
40. Yang, P.; Lai, D.Y.; Jin, B.; Bastviken, D.; Tan, L.; Tong, C. Dynamics of dissolved nutrients in the aquaculture shrimp ponds of the Min River estuary, China: Concentrations, fluxes and environmental loads. *Sci. Total Environ.* **2017**, *603*, 256–267. [[CrossRef](#)] [[PubMed](#)]
41. Funge-Smith, S.J.; Briggs, M.R. Nutrient budgets in intensive shrimp ponds: Implications for sustainability. *Aquaculture* **1998**, *164*, 117–133. [[CrossRef](#)]
42. Hansen, H.P.; Koroleff, F. Determination of nutrients. In *Methods of Seawater Analysis*; Grasshoff, K., Kremling, K., Ehrhardt, M., Eds.; WILEY-VCH: Weinheim, Germany, 1999; pp. 159–288, ISBN 3-527-29589-5.
43. Liu, S.M.; Zhang, J.; Chen, H.T.; Wu, Y.; Xiong, H.; Zhang, Z.F. Nutrients in the Changjiang and its tributaries. *Biogeochemistry* **2003**, *62*, 1–18. [[CrossRef](#)]
44. Cai, Y.H.; Guo, L.D. Abundance and variation of colloidal organic phosphorus in riverine, estuarine, and coastal waters in the northern Gulf of Mexico. *Limnol. Oceanogr.* **2009**, *54*, 1393–1402. [[CrossRef](#)]
45. Yang, B.; Cao, L.; Liu, S.M.; Zhang, G.S. Biogeochemistry of bulk organic matter and biogenic elements in surface sediments of the Yangtze River Estuary and adjacent sea. *Mar. Pollut. Bull.* **2015**, *96*, 471–484. [[CrossRef](#)] [[PubMed](#)]
46. Aspila, K.I.; Agemian, H.; Chau, A.S.Y. A semi-automated method for the determination of inorganic, organic and total phosphate in sediments. *Analyst* **1976**, *101*, 187–197. [[CrossRef](#)] [[PubMed](#)]
47. Parsons, T.R.; Maita, Y.; Lalli, C.M. A manual for Chemical and Biological Methods for Seawater Analysis. Pergamon Press: Oxford, UK, 1984; p. 173, ISBN 0-08-030288-2.
48. Kaiser, H.F. The application of electronic computers to factor analysis. *Educ. Psychol. Meas.* **1960**, *20*, 141–151. [[CrossRef](#)]
49. Gopinath, A.; Joseph, N.; Sujatha, C.H.; Nair, S.M. Forms of Nitrogen (NO<sub>3</sub>-N; NO<sub>2</sub>-N and NH<sub>2</sub>CONH<sub>2</sub>-N) and their relations to A.O.U in the Indian coastal waters of Arabian Sea. *Chem. Ecol.* **2002**, *18*, 233–244. [[CrossRef](#)]
50. Durga Rao, G.; Kanuri, V.V.; Kumaraswami, M.; Ezhilarasan, P.; Rao, V.D.; Patra, S.; Dash, S.K.; Peter, M.; Rao, V.R.; Ramu, K. Dissolved nutrient dynamics along the southwest coastal waters of India during northeast monsoon: A case study. *Chem. Ecol.* **2017**, *33*, 229–246. [[CrossRef](#)]

51. Justić, D.; Rabalais, N.N.; Turner, R.E.; Dortch, Q. Changes in nutrient structure of river-dominated coastal waters: Stoichiometric nutrient balance and its consequences. *Estuar. Coast. Shelf Sci.* **1995**, *40*, 339–356. [[CrossRef](#)]
52. Shim, M.J.; Swarzenski, P.W.; Shiller, A.M. Dissolved and colloidal trace elements in the Mississippi River delta outflow after Hurricanes Katrina and Rita. *Cont. Shelf Res.* **2012**, *42*, 1–9. [[CrossRef](#)]
53. Baker, D.B.; Confesor, R.; Ewing, D.E.; Johnson, L.T.; Kramer, J.W.; Merryfield, B.J. Phosphorus loading to Lake Erie from the Maumee, Sandusky and Cuyahoga rivers: The importance of bioavailability. *J. Great Lakes Res.* **2014**, *40*, 502–517. [[CrossRef](#)]
54. Van der Zee, C.; Roevros, N.; Chou, L. Phosphorus speciation, transformation and retention in the Scheldt estuary (Belgium/The Netherlands) from the freshwater tidal limits to the North Sea. *Mar. Chem.* **2007**, *106*, 76–91. [[CrossRef](#)]
55. Lin, P.; Chen, M.; Guo, L.D. Speciation and transformation of phosphorus and its mixing behavior in the Bay of St. Louis estuary in the northern Gulf of Mexico. *Geochim. Cosmochim. Acta* **2012**, *87*, 283–298. [[CrossRef](#)]
56. Cai, Y.H.; Guo, L.D.; Douglas, T.A.; Whitedge, T.E. Seasonal variations in nutrient concentrations and speciation in the Chena River, Alaska. *J. Geophys. Res. Biogeosci.* **2008**, *113*, G030035. [[CrossRef](#)]
57. Guo, L.D.; Zhang, J.Z.; Guéguen, C. Speciation and fluxes of nutrients (N, P, Si) from the upper Yukon River. *Glob. Biogeochem. Cycles* **2004**, *18*, GB1038. [[CrossRef](#)]
58. Guo, L.D.; Cai, Y.H.; Belzile, C.; Macdonald, R.W. Sources and export fluxes of inorganic and organic carbon and nutrient species from the seasonally ice-covered Yukon River. *Biogeochemistry* **2012**, *107*, 187–206. [[CrossRef](#)]
59. Ho, A.Y.; Xu, J.; Yin, K.D.; Jiang, Y.L.; Yuan, X.C.; He, L.; Anderson, D.M.; Lee, J.H.W.; Harrison, P.J. Phytoplankton biomass and production in subtropical Hong Kong waters: influence of the Pearl River outflow. *Estuar. Coast.* **2010**, *33*, 170–181. [[CrossRef](#)]
60. Zhang, J.Z.; Huang, X.L. Effect of temperature and salinity on phosphate sorption on marine sediments. *Environ. Sci. Technol.* **2011**, *45*, 6831–6837. [[CrossRef](#)] [[PubMed](#)]
61. Brooks, A.S.; Edgington, D.N. Biogeochemical control of phosphorus cycling and primary production in Lake Michigan. *Limnol. Oceanogr.* **1994**, *39*, 961–968. [[CrossRef](#)]
62. Lean, D.R.S. Phosphorus dynamics in lake water. *Science* **1973**, *179*, 678–680. [[CrossRef](#)] [[PubMed](#)]
63. Qin, X.L.; Chen, B.; Lai, J.X.; Lu, J.C.; Ya, H.Z. Study on the utilization of different phosphorus and alkaline phosphatase characteristics of *Phaeocystis globosa* cultivated from Beibu Gulf. *Guangxi Sci.* **2018**, *25*, 80–86. (In Chinese)
64. Yoshimura, T.; Nishioka, J.; Saito, H.; Takeda, S.; Tsuda, A.; Wells, M.L. Distributions of particulate and dissolved organic and inorganic phosphorus in North Pacific surface waters. *Mar. Chem.* **2007**, *103*, 112–121. [[CrossRef](#)]
65. Li, R.H.; Liu, S.M.; Li, Y.W.; Zhang, G.L.; Ren, J.L.; Zhang, J. Nutrient dynamics in tropical rivers, lagoons, and coastal ecosystems of eastern Hainan Island, South China Sea. *Biogeosciences* **2014**, *11*, 481–506. [[CrossRef](#)]
66. Senthikumar, B.; Purvaja, R.; Ramesh, R. Seasonal and tidal dynamics of nutrients and chlorophyll a in a tropical mangrove estuary, southeast coast of India. *Indian J. Mar. Sci.* **2008**, *37*, 132–140.
67. Burford, M.A.; Rothlisberg, P.C. Factors limiting phytoplankton production in a tropical continental shelf ecosystem. *Estuar. Coast. Shelf Sci.* **1999**, *48*, 541–549. [[CrossRef](#)]
68. Lin, P.; Klump, J.V.; Guo, L.D. Dynamics of dissolved and particulate phosphorus influenced by seasonal hypoxia in Green Bay, Lake Michigan. *Sci. Total Environ.* **2016**, *541*, 1070–1082. [[CrossRef](#)] [[PubMed](#)]

